



Evaluation of the effect of anisotropic consolidation and principle stress rotation on undrained behavior of silty sands

R. Keyhani and S.M. Haeri*

School of Civil Engineering, Sharif University of Technology, Tehran, Iran.

Received 16 September 2012; received in revised form 6 January 2013; accepted 12 March 2013

KEYWORDS

Hollow cylinder test;
Anisotropic behavior;
Silty sand;
Pore water pressure;
Undrained behavior.

Abstract. The dependence of undrained behavior of silty sand on initial state of stress and direction of principal stresses with respect to vertical (α) is assessed under generalized loading paths using hollow cylinder apparatus. During applying shear load, value of intermediate principal stress parameter (b) is held constant and α value is increased from zero to the aimed value and held constant. Specimens are consolidated, both, isotropically and anisotropically to evaluate the effect anisotropic consolidation on the behavior of these soils. The wet tamping method was selected to prepare specimen. Shear loading was carried out under strain-controlled condition to capture post-peak strain-softening response. The results of this study reveal that the principal stress direction and initial anisotropy in stress condition have considerable effects on the behavior of silty sands. By increasing α , susceptibility of silty sand to instability increases. In addition, increase in silt content of silty sand mixtures presents higher tendency to flow compared to pure sand. For specimens with high silt content, it is observed that stress-strain response has a sudden reduction in shear strength after a peak. This study reveals that shear strength and steady state friction angle of the silty sands are affected by α and the amount of fines present in the sand.

© 2013 Sharif University of Technology. All rights reserved.

1. Introduction

Initial direction of major principle stress in natural horizontal layers of soils is usually vertical. However applying shear load by excavation, embankment, foundation of structures and wave load in sea bed layer causes rotation of principal stress direction. The directions of principal stresses in triaxial tests are fixed and can only rotate at 90° . However the Hollow Cylinder Apparatus (HCA) provides a convenient way of assessing influence of rotation of principal stress direction on the behavior of soils including silty sands [1].

The role of non-plastic silt on stress-strain behavior of loose sand has been under discussion for

decades. Terzaghi [2] hypothesized that silt particles could create a “metastable” structure that could explain the static liquefaction observed during failure of large submarine slopes. Recent laboratory studies on susceptibility of liquefaction appear to be divided regarding the effect of non-plastic silt content. Kuerbis et al. [3] observed that increasing silt content up to 20% resulted in more dilative behavior of sand in undrained triaxial tests when the tests were performed at the same skeleton void ratio. Pitman et al. [4] also concluded that when silt was added to Ottawa sand, it became less collapsible in undrained triaxial compression tests. Ishihara [5] and Verdugo and Ishihara [6] have found that non-plastic silt may increase the potential of liquefaction. They concluded that increasing silt content causes a contractive behavior that can induce the possibility of flow failure or liquefaction. Amini and

*. Corresponding author. Fax: +98 21 66014828
E-mail address: smhaeri@sharif.edu (S.M. Haeri)

Qi [7] reported that fine content increased resistance to liquefaction of sand during cyclic tests. Lade and Yamamuro [8] and Yamamuro and Lade [9], observed that increasing non-plastic silt content in Nevada sand increased the contractive behavior of a specimen in both drained and undrained triaxial tests, even when density was increased. Thevanayagam [10] found that the presence of non-plastic silt may either increase or decrease undrained shear strength depending on the intergranular void ratio [11,12].

The experimental data for specimens at the same void ratio indicate that steady-state shear strength decreases initially by increasing fines content, but when fines content increase beyond about 30%, steady-state shear strength starts to increase [5,4,13].

The overall response of the mixed soils at different percentages of fines is investigated by Yang and Wei [14]. One of the significant findings is that the critical state friction angle of a mixed soil is affected not only by the shape of coarse particles but also by the shape of fine particles, and this shape effect is coupled with fines content.

Many tests by HCA have been performed to prove the effect of anisotropy on the behavior of sands [15–17]. The inherent anisotropy effect in Toyoura sand has been studied by Yoshimine et al. [15] for different directions of major principal stress. When direction of major principal stress with respect to vertical (α) becomes larger, the behavior of material clearly softens and shows to be more contractive. As reported by Yoshimine et al. [15], under loading in the case of $\alpha = 15^\circ$, a hardening behavior with only 20% excess pore water pressure ratio was developed. Whereas, in case of $\alpha = 75^\circ$, pore water pressure ratio was developed up to nearly 90%, and there was a strong strain softening in behavior. Similar results have been reported by Sivathayalan and Vaid [16] and Uthayakumar and Vaid [17]. Difference in the results of conventional triaxial compression and extension tests on sands also, to some extent, reveal the inherent anisotropy in sands. Although the compression tests have been generally used for undrained monotonic loading in large deformation (e.g. [5,6]), a few researchers have pointed out that the undrained shear behavior of sand in extension tests is far more contractive than that in compression tests [15]. This fact proves the effect of anisotropy in sand using triaxial apparatus.

The role of initial static shear stress in liquefaction resistance is studied by Yang and Sze [18]. The presence of initial static shear stress is beneficial to the liquefaction resistance of loose sand at low initial shear stress ratio, but it becomes detrimental at high α levels. The initial static shear stress is an important factor in the softening behavior during the shear loading of loose sand. Sivathayalan and Vaid [16] showed that the minimum undrained strength of the strain-softening

sand is found to be highly influenced by the initial stress state, even though the friction angle mobilized at the instant of minimum strength is unique. Also Kato et al. [19] specified that the relation between void ratio and confining stress at steady state and quasi-steady state are independent of the extent of anisotropic consolidation. However different states of consolidation stress were shown to affect the stress-strain behavior of sand and the development of excess pore water pressure up to an axial strain of 5%. Additionally, Sladen et al. [20] indicated that anisotropically consolidated samples often failed in undrained triaxial monotonic tests, when the stress state reached the collapse surface obtained from isotropic tests.

This paper presents an experimental study of the static undrained response of silty sand specimen reconstituted by wet tamping in a Hollow Cylinder Apparatus under different directions of major principle stress (α). The main objective of this study is to assess the dependence of the behavior of silty sands on initial anisotropic stress state, in addition to the direction of major principle stress. The tests were conducted on sand samples containing 0, 10, 30 and 40% silt content (f_c). Similar preparation method, effective consolidation stress, and laboratory procedure were used for each specimen. The results of the tests on specimens with almost similar relative density are compared and discussed.

2. Tested material

The tests in this experimental program were on Babolsar sand which is a standard sand in Iran and is classified as SP according to the Unified Soil Classification System [21]. The non-plastic silt was obtained by grinding local natural alluvium deposits of sand and gravel. This paper studies four mixtures of Babolsar sand with 0%, 10%, 30% and 40% by weight of non-plastic silt. The grain size distribution curves of the mixtures are shown in Figure 1. The uniformity coefficient C_u and the mean grain size D_{50}

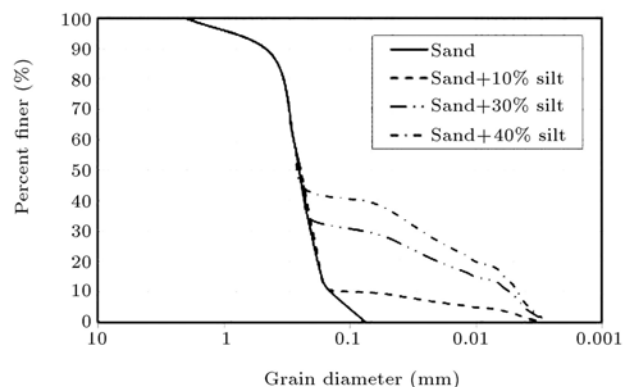


Figure 1. Grain size distribution curves.

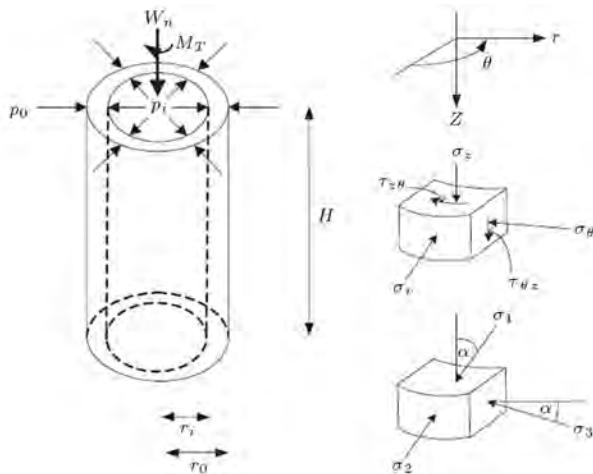
Table 1. Specific gravity and minimum and maximum void ratios for sand-silt mixtures.

Silt content (%)	G_s	e_{\max}	e_{\min}
0	2.75	0.790	0.530
10	2.74	0.768	0.510
30	2.73	0.720	0.462
40	2.73	0.810	0.499

of sand were found to be equal to 2.00 and 0.23 mm respectively. The maximum and minimum void ratios and the specific gravity of soil solids (G_s) of the sand-silt mixtures respectively are provided in Table 1. The specific gravity of silt material is also 2.68.

3. Hollow cylinder apparatus

The tests were performed using the HCA at Advanced Soil Mechanics Laboratory of Sharif University of Technology. The device is capable of subjecting an axial load (W_n), a torque (M_T) about the central vertical axis, and different external pressure (P_o) and internal pressure (P_i) to a hollow cylindrical specimen of soil (see Figure 2). These surface tractions are independently controlled using automatic stress path loading, thus enabling the loading of a specimen of soil along a prescribed stress path in the general four-dimensional effective stress space described by vertical normal stress (σ_z), circumferential normal stress (σ_θ), radial normal stress (σ_r) and shear stress ($\tau_{z\theta}$) (see Figure 2). Alternatively, the same stress state can be represented in terms of magnitudes and directions of three principal effective stresses σ'_1 , σ'_2 , σ'_3 and angle of major principal effective stress with respect to vertical (α). The initial stress ratio $k_c = (\sigma'_3/\sigma'_1)$, effective mean normal stress $P' = (\sigma'_1 + \sigma'_2 + \sigma'_3)/3$ and intermediate principal stress parameter $b = (\sigma'_2 - \sigma'_3)/(\sigma'_1 - \sigma'_3)$ are also frequently used as they are

**Figure 2.** Element component and principle stresses.

believed to be key stress variables that influence on the behavior of sand and silty sand.

Stress and strain gradients exist across the wall of a hollow cylinder specimen due to its shape and end restraint. Tests were controlled and interpreted in terms of average stresses and strains induced in specimen during loading [22]. The average stresses are defined as:

$$\sigma_z = \frac{W_n}{\pi(r_o^2 - r_i^2)} + \frac{P_o \cdot r_o^2 - P_i \cdot r_i^2}{(r_o^2 - r_i^2)}, \quad (1)$$

$$\sigma_r = \frac{P_o \cdot r_o + P_i \cdot r_i}{(r_o + r_i)}, \quad (2)$$

$$\sigma_\theta = \frac{P_o \cdot r_o - P_i \cdot r_i}{(r_o - r_i)}, \quad (3)$$

$$\tau_{z\theta} = \frac{3 \cdot M_T}{2\pi(r_o^3 - r_i^3)}, \quad (4)$$

in which r_o and r_i are the external and internal specimen radii respectively.

Principle stress components can be calculated by using Mohr's circle based on values of average stresses. Radial normal stress is equal to intermediate principle stress. So, the maximum and minimum principle stresses and α can be derived by the following formulas:

$$\sigma_{1,3} = \frac{\sigma_z + \sigma_\theta}{2} \pm \sqrt{\left(\frac{\sigma_z - \sigma_\theta}{2}\right)^2 + \tau_{z\theta}^2}, \quad (5)$$

$$q = \sigma_1 - \sigma_3 = 2\sqrt{\left(\frac{\sigma_z - \sigma_\theta}{2}\right)^2 + \tau_{z\theta}^2}, \quad (6)$$

$$\alpha = \frac{1}{2} \tan^{-1} \left(\frac{2\tau_{z\theta}}{\sigma_z - \sigma_\theta} \right). \quad (7)$$

4. Specimen preparation and testing procedure

4.1. Specimen preparation

The specimens tested had outer diameter of 100 mm, inner diameter of 60 mm and a height of approximately 200 mm. These dimensions ensure a middle height zone in the specimen that remains unaffected by boundary conditions [23].

In this study, the wet tamping method was implemented for specimen preparation using under-compaction procedure proposed by Ladd [24]. The selected method was the most suitable method to obtain a very loose state of soil packing and a good procedure for building fairly uniform reconstituted specimens [5]. Initial water contents range from 5% to 8% for different silt contents in order to obtain specimens with allocated relative density.

The density of soil after consolidation is a very important parameter in the behavior of soils. Soils with higher density show more dilative response. It is common to use void ratio for clean sands. In mixed soils, like silty sand, the controlling density condition differs from clean sands. As reported in Table 1, the minimum and maximum void ratios are not constant for different silt contents. So it is not appropriate to compare the behavior of a silty soil with that of a clean sand using global void ratio (e) or any other solid density parameter. Sand and sand-silt mixes are expected to show similar mechanical behavior, if compared at the same contact density index. A soil classification system, based on contact density, has been developed by Thevanayagam et al. [25] and Thevanayagam [26]. The relevant equivalent intergranular $e_{c(eq)}$ and relevant equivalent interfine $e_{f(eq)}$ contact density indices have been introduced as:

$$e_{c(eq)} = \frac{e + (1 - b_i)f_c}{1 - (1 - b_i)f_c}, \quad (8)$$

$$e_{f(eq)} = \frac{e}{f_c + \frac{1-f_c}{R_d^m}}. \quad (9)$$

Both b_i and m are empirical values. Parameter b_i denotes the portion of the fine grains that contributes to the active intergrain contacts and statistically is about 0.25. Parameter m is reinforcement factor and according to the reported studies by Thevanayagam et al. [25], it is about 0.65. Also parameter R_d is particle size disparity ratio ($D_{50(\text{sand})}/d_{50(\text{silt})}$) and in our case is equal 26.

As mentioned, the specimens with different silt contents should have the same contact density index to show similar behavior. However preparing samples with the same $e_{c(eq)}$ for soils with silt contents is very difficult and somehow impossible. So in this study, because of the wide variation of the tested sand-silt mixtures, the intergranular and interfine void ratio cannot be fixed for different silt contents and cannot be adopted as controlling density indices despite a possible better interpretation of the problem (Table 2). Relative density (D_r) is a more common and suitable index property for comparing undrained behavior of specimens with different silt percentages [11,12].

During and after saturation and consolidation stages, the volume of the specimens decrease considerably [12]. Therefore preparing hollow specimens of high silt content with low relative density is very difficult. Practically, it seems that it is not possible to prepare mixed soils with a broad range of silt content with equal relative densities after consolidation. In this study, specimens with different silt contents are prepared with similar preparation method in the lowest possible relative densities. Thus, for example, when the

relative density of the pure sand is about 40% after consolidation, the relative density of less than 50% cannot be obtained for silty sand with 40% silt and the same specimen preparation method.

4.2. Saturation

After the specimen was prepared by wet tamping method, a hydrostatic pressure of 20 kPa applied on the specimen and vacuum was removed from around the specimen and carbon dioxide gas was circulated from the bottom to the top of the specimen for 30 minutes. Test specimens were initially saturated by flushing deaired water from the base of the specimen. Then a back pressure was applied to ensure water saturation with Skempton's B value exceeding 0.95. A small amount of silt migration was noted in samples with large fine contents.

4.3. Consolidation

Isotropic consolidation was attained by increasing both axial and lateral stresses with the same amount simultaneously. In contrast, anisotropic consolidation with initial stress ratio $k_c = \sigma'_{3c}/\sigma'_{1c}$ other than unity was achieved by raising both axial stress (σ'_{1c}) and lateral stress (σ'_{3c}) simultaneously, while maintaining k_c equal to the desired value during consolidation stage. In anisotropic consolidation, the intermediate principal stress parameter (b) and mean effective stress (p') should be controlled, as well, to be able to define appropriate stress path. In the present study the specimens are consolidated with k_c equal 0.33, 0.5 and 1 to study the effect of anisotropic consolidation on the behavior of sands and silty sands.

4.4. Stress path

After completed consolidation, undrained loading was applied in a strain-controlled manner with an axial strain rate of 0.5% per minute. In order to study the anisotropic consolidation effect, b is planned to be held constant during each test. In the end of consolidation stage, α is equal zero except for isotropic consolidation condition. So, α should be increased from zero to the aimed value during shear loading. However it is increased fast during the initial stage of shear loading and then it is held constant.

According to Verdugo and Ishihara [6], estimation of void ratio of specimen in consolidation stage based on water content is more accurate and has less statistical scatter than that estimated based on initial specimen dimensions and measured volume changes during consolidation.

Membrane penetration was not taken into account since the sand and silty sand used in this experiment were fine to medium sand and silty sand. In addition, visual observation of the specimens throughout the tests indicated that membranes were smooth with no visual indication of penetration.

Table 2. Summary of test result.

No.	Silt content (%)	α (deg.)	K_c	e (void ratio at the end of consolidation)	Relative density (%)	$e_{c(eq)}$	$e_{f(eq)}$	q_{peak} (kPa)	q_{min} (kPa)
1	0	20	1	0.683	41	0.683	5.54	-	-
2	0	40	1	0.686	40	0.686	5.56	-	-
3	0	60	1	0.681	42	0.681	5.52	-	-
4	0	80	1	0.681	42	0.681	5.52	128.0	96.2
5	10	20	1	0.660	42	0.794	3.13	-	-
6	10	40	1	0.652	45	0.786	3.09	-	-
7	10	60	1	0.657	43	0.791	3.11	130.0	85.0
8	10	80	1	0.657	43	0.791	3.11	118.0	65.0
9	30	20	1	0.596	48	1.060	1.54	130.0	85.8
10	30	40	1	0.591	50	1.053	1.53	120.0	70.1
11	30	60	1	0.591	50	1.053	1.53	108.0	45.1
12	30	80	1	0.594	49	1.056	1.54	102.0	37.9
13	40	20	1	0.651	51	1.359	1.37	142.8	103.9
14	40	40	1	0.648	52	1.355	1.37	127.8	81.2
15	40	60	1	0.655	50	1.364	1.38	114.9	60.5
16	40	80	1	0.642	54	1.346	1.35	108.2	44.7
17	0	20	0.5	0.681	42	0.681	5.52	-	-
18	0	40	0.5	0.683	41	0.683	5.54	-	-
19	0	60	0.5	0.686	40	0.686	5.56	-	-
20	0	80	0.5	0.681	42	0.681	5.52	180.0	143.5
21	10	20	0.5	0.657	43	0.791	3.11	-	-
22	10	40	0.5	0.660	42	0.794	3.13	-	-
23	10	60	0.5	0.665	40	0.800	3.15	174.0	119.9
24	10	80	0.5	0.652	45	0.786	3.09	170.0	101.8
25	30	20	0.5	0.591	50	1.053	1.53	170.0	112.9
26	30	40	0.5	0.596	48	1.060	1.54	160.0	95.9
27	30	60	0.5	0.591	50	1.053	1.53	148.0	66.2
28	30	80	0.5	0.599	47	1.063	1.55	143.0	54.3
29	40	20	0.5	0.651	51	1.359	1.37	181.2	128.0
30	40	40	0.5	0.639	55	1.341	1.35	167.0	110.5
31	40	60	0.5	0.658	49	1.368	1.39	153.6	79.1
32	40	80	0.5	0.645	53	1.350	1.36	150.0	67.2
33	0	20	0.33	0.683	41	0.683	5.54	-	-
34	0	40	0.33	0.683	41	0.683	5.54	-	-
35	0	60	0.33	0.681	42	0.681	5.52	-	-
36	0	80	0.33	0.678	43	0.678	5.50	232.0	181.8
37	10	20	0.33	0.657	43	0.791	3.11	-	-
38	10	40	0.33	0.657	43	0.791	3.11	-	-
39	10	60	0.33	0.662	41	0.797	3.14	226.0	151.6
40	10	80	0.33	0.660	42	0.794	3.13	222.0	128.5
41	30	20	0.33	0.594	49	1.056	1.54	222.0	144.9
42	30	40	0.33	0.594	49	1.056	1.54	216.0	122.4
43	30	60	0.33	0.588	51	1.050	1.52	212.0	94.5
44	30	80	0.33	0.596	48	1.060	1.54	210.0	74.7
45	40	20	0.33	0.655	50	1.364	1.38	225.3	165.1
46	40	40	0.33	0.645	53	1.350	1.36	218.8	141.5
47	40	60	0.33	0.642	54	1.346	1.35	214.7	110.0
48	40	80	0.33	0.648	52	1.355	1.37	211.5	94.0

All of the tests were performed along the stress paths shown in Figure 3 by controlling the internal and external pressures, the vertical load and the torque, as explained previously. Figure 3 shows the normalized shear stress ($\tau_{z\theta}/P'_c$) against the normalized deviator stress ($(\sigma_z - \sigma_r)/P'_c$), where P'_c is the initial confining pressure. As shown in Figure 3(a) to (c), stress paths of specimens with different anisotropic consolidation conditions are the same and only the initial stress state of shear loading is different.

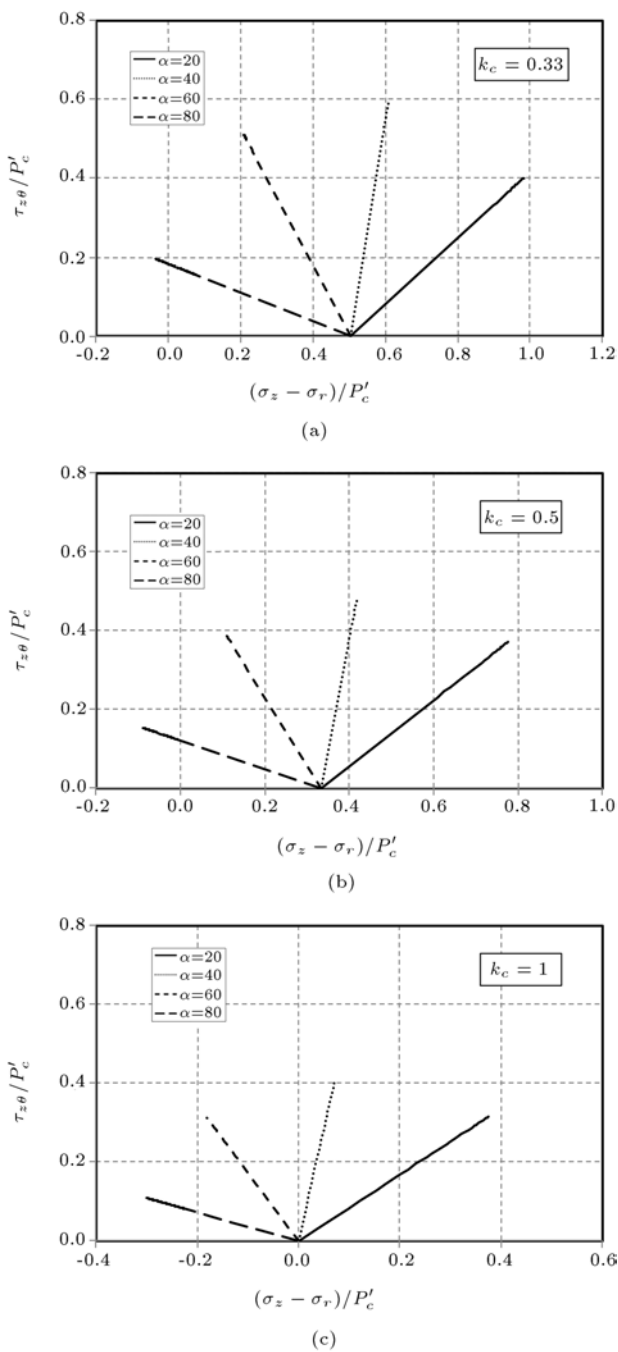


Figure 3. Stress paths employed on silty sand specimens with isotropic and anisotropic consolidation.

5. Type of tests performed and results

Forty eight undrained shear tests were conducted with constant value of b during shear stage of each test as depicted in Table 2. The tests were carried out on sand and silty sand consolidated to almost identical relative densities. The tests were carried out to study the effect of initial stress states characterized by k_c and α and various silt percentages on the behavior of silty sands. A constant effective mean normal consolidation stress (p'_c) of 200 kPa and $b = 0.5$ was used in all tests.

5.1. Test results

For a systematic quantification of undrained behavior of the studied silty soil, following three states were distinguished: the steady state, the quasi-steady state and the phase transformation state [27,28]. These states are discussed next for the test results of this study.

The steady state is the state at which the soil deforms at constant effective stresses (i.e. zero change in q and p) and constant void ratio in drained tests and constant pore water pressure in undrained tests. However, in experiments, there are small deviations from these ideal conditions. The steady state usually happens for sand with high silt content when it is sheared in a high α value. The quasi-steady state (QSS) is defined as the state at which the Deviatoric Stress q reaches a local minimum in undrained shearing. Experimental results show that the QSS constitutes a distinct soil state. The phase transformation is the state at which contractive behavior changes to dilative one and usually occurs without losing the strength at that state. In pure sand samples especially in small α value a distinct phase transformation could be observed.

The results of the tests on sand and silty sand materials are shown in Figures 4 to 15 for $k_c = 0.33$, 0.5 and 1 and $\alpha = 20^\circ$, 40° , 60° and 80° . Figures 4 to 6 include the results of a package of tests on clean sand. The relative densities (D_r) of the samples were in a range of 41% to 42% after consolidation and the initial confining stress was 200 kPa. It can be noticed from Figures 4 to 6 that, by increasing α , the behavior becomes clearly softer and more contractive and pore water pressure increases during undrained shear. In the tests with $\alpha = 20^\circ$ the behavior was completely dilative and softening behavior did not occur, whereas in the tests with $\alpha = 80^\circ$ Quasi Steady State was obvious. The stress path and stress-strain curves of the tests with $\alpha = 40^\circ$ and $\alpha = 60^\circ$ also have dilative behavior. Such a systematic softening (with α) has been attributed to change in loading condition from compression ($\alpha = 20^\circ$) to extension ($\alpha = 80^\circ$).

The comparative behavior of sand consolidated with identical α and different k_c values can be observed from Figures 4 to 6. As can be observed, the sand material does not exhibit strain softening at $\alpha = 20^\circ$

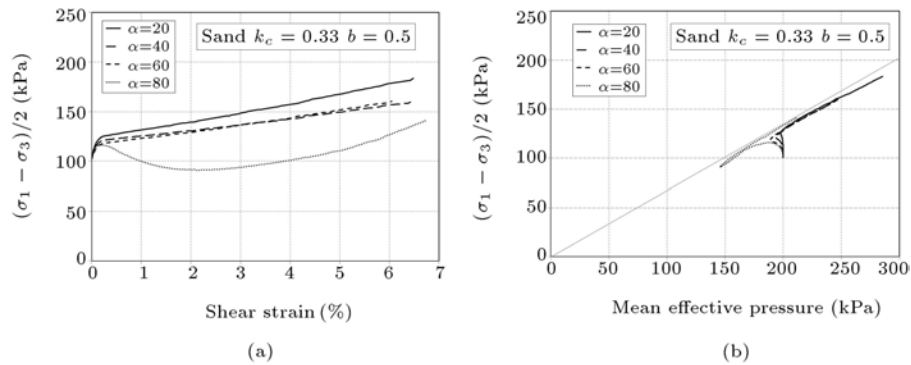


Figure 4. Effect of α on the behavior of Babolsar sand in $P'_c = 200$ kPa and $k_c = 0.33$.

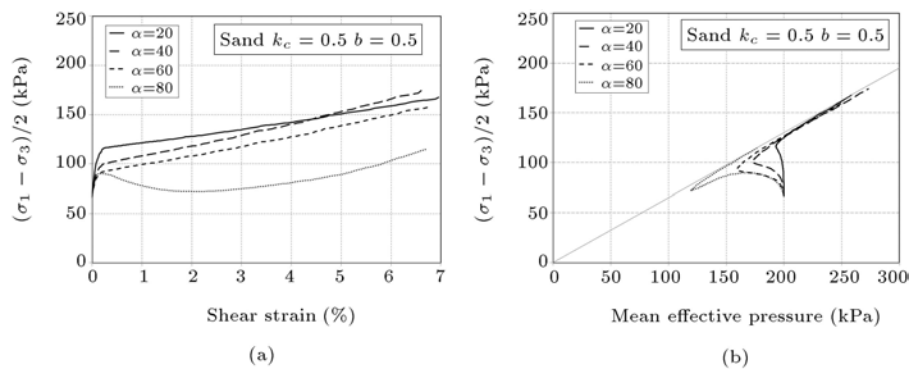


Figure 5. Effect of α on the behavior of Babolsar sand in $P'_c = 200$ kPa and $k_c = 0.5$.

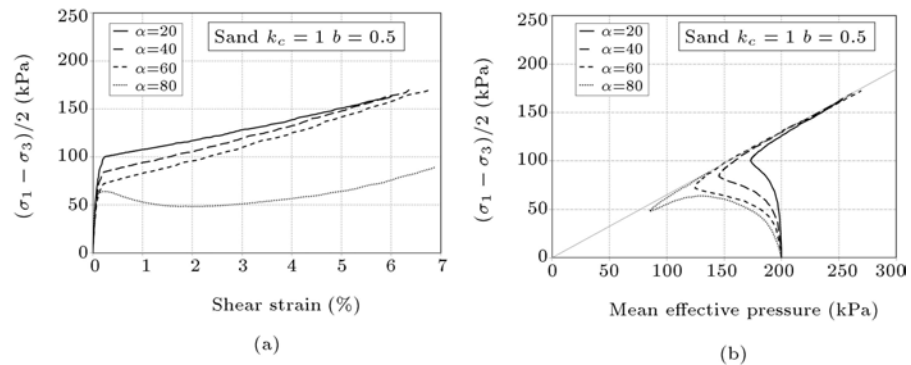


Figure 6. Effect of α on the behavior of Babolsar sand in $P'_c = 200$ kPa and $k_c = 1$.

and 40° for all k_c values. But it appears for shear loading with $\alpha = 60^\circ$ and 80° that the behavior of specimens become marginally less strain softening by increasing anisotropy in consolidation (decreasing k_c); although the difference is relatively minor.

As mentioned before and shown in Figures 4 to 6, the behavior of sand specimen changes from strain hardening to strain softening when α increases. Also deviatoric stresses increase by increasing shear strain, so it seems there is no tendency to reach a steady state for the sand specimens. Consolidating specimen with lower k_c (higher anisotropy) causes the sand samples to behave more dilative in contrast to the specimen consolidated isotropically.

The stress path of shear stress for specimens with 10% silt is shown in Figures 7 to 9. The relative densities of specimens were in the range of 40% to 45% and the initial mean effective stress was 200 kPa. By increasing α , the behaviors of specimens change from dilative to strain softening. The specimens have dilative behavior at $\alpha = 20^\circ$ and 40° . But for $\alpha = 60^\circ$, the specimen exhibits a dilative behavior in the initial stage of shear, and the shear strength of the specimen decreased and reached to a local minimum value (QSS), however the shear strength increased again by increasing the shear strain indicating a phase-transformation. The strength of specimens with 10% silt decreases from that of the sand specimens.

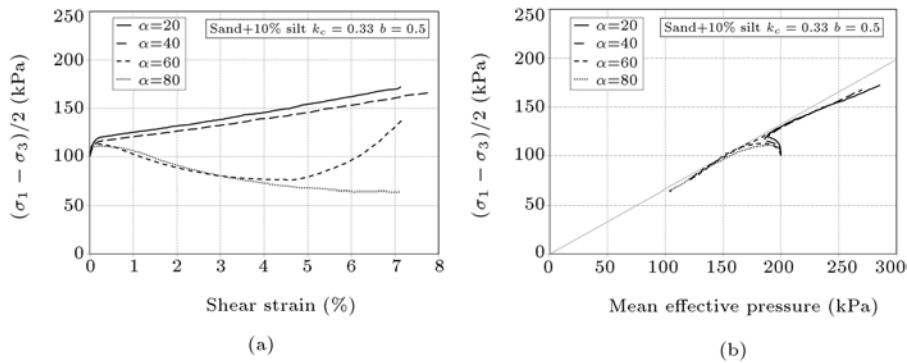


Figure 7. Effect of α on the behavior of Babolsar sand with 10% silt in $P'_c = 200$ kPa and $k_c = 0.33$.

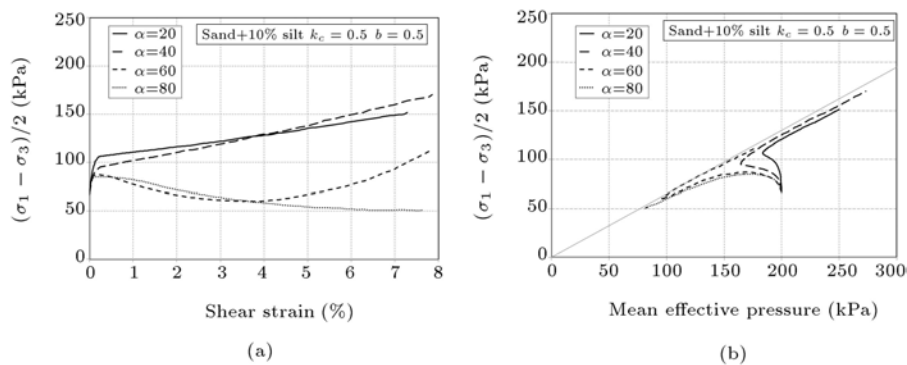


Figure 8. Effect of α on the behavior of Babolsar sand with 10% silt in $P'_c = 200$ kPa and $k_c = 0.5$.

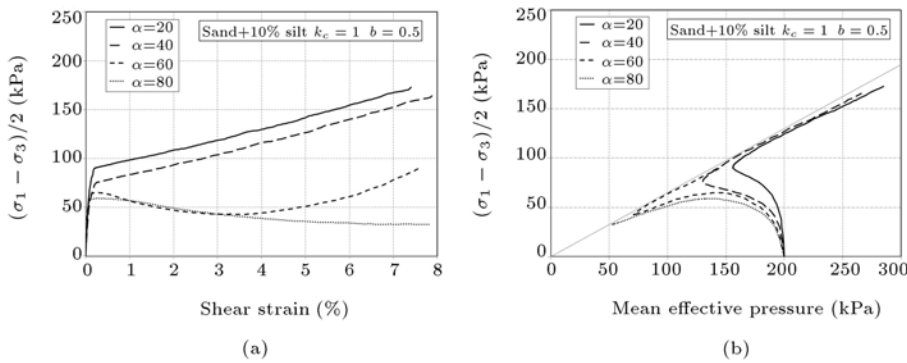


Figure 9. Effect of α on the behavior of Babolsar sand with 10% silt in $P'_c = 200$ kPa and $k_c = 1$.

Figures 10 to 12 show the test results for silty sand material with 30% silt. As shown in these figures, the behavior of the material becomes more contractive and shear strength decrease by adding silt content in the specimens. Adding non-plastic silt to the host sand made it much more susceptible to strain softening. It can be observed in the Figures 10 to 12 that all of the specimens have a similar strain softening behavior for all α and k_c value and for silt content of 30%.

The test results for specimens with 40% silt are shown in Figures 13 to 15. The relative densities of tested specimens are 49% to 55%. As depicted, the shear strength of these specimens decreases with respect to that of sand specimen but they increase with

respect to the shear strength of sand with 30% silt. That is, adding silt to sand material initially decreases shear strength and then increases it when silt contents are beyond a threshold value. As mentioned by Murthy et al. [29], this phenomenon is very important because it seems that bearing skeleton of sand is being changed to silt skeleton. In this condition, silt skeleton dominates and the sand grains are in silty skeleton without any contact of sand grain. In the lower amount of silt content, the silt material does not have a separate skeleton and only fills the voids of the sand skeleton. It seems that the particles of silty material lubricate moving the sand grains and reduce the strength of interparticle contacts. As a result, the strength of silty

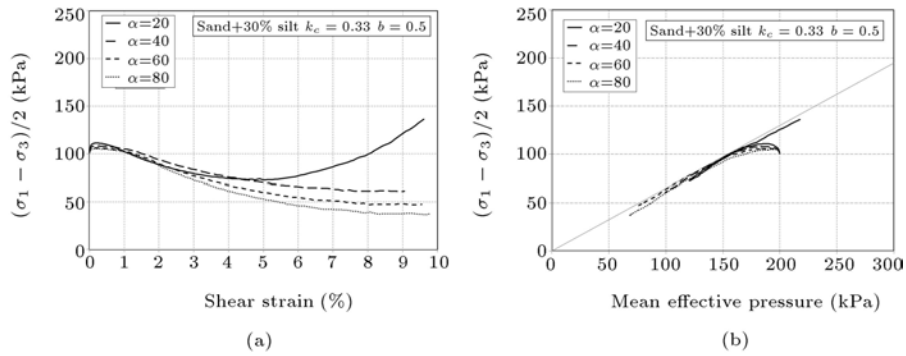


Figure 10. Effect of α on the behavior of Babolsar sand with 30% silt in $P'_c = 200$ kPa and $k_c = 0.33$.

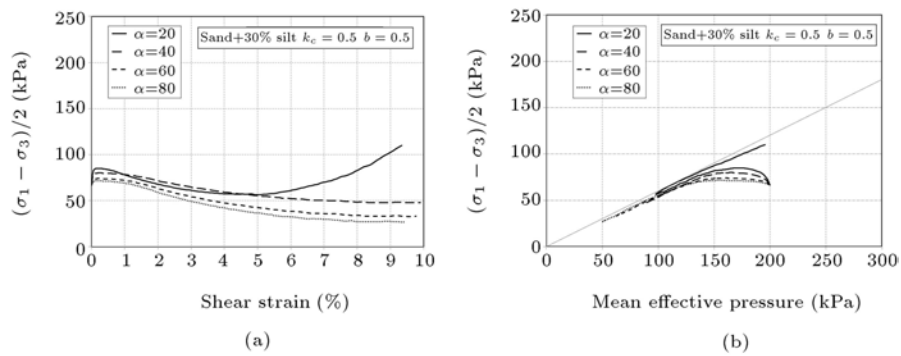


Figure 11. Effect of α on the behavior of Babolsar sand with 30% silt in $P'_c = 200$ kPa and $k_c = 0.5$.

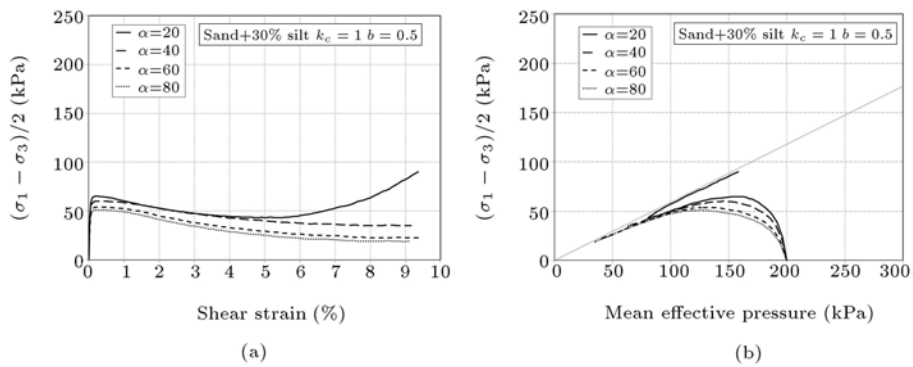


Figure 12. Effect of α on the behavior of Babolsar sand with 30% silt in $P'_c = 200$ kPa and $k_c = 1$.

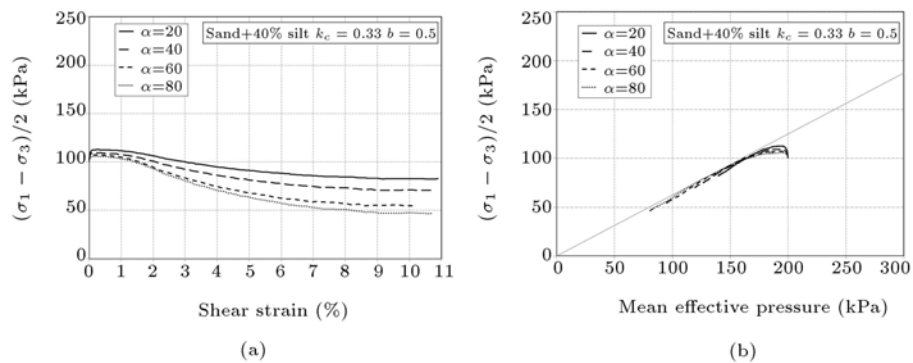


Figure 13. Effect of α on the behavior of Babolsar sand with 40% silt in $P'_c = 200$ kPa and $k_c = 0.33$.

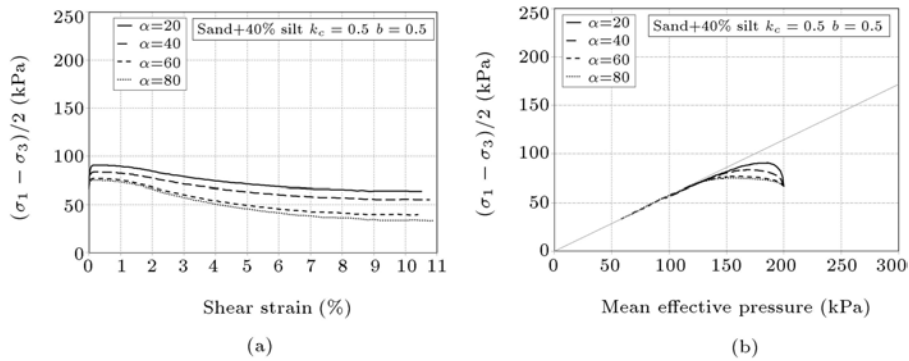


Figure 14. Effect of α on the behavior of Babolsar sand with 40% silt in $P'_c = 200$ kPa and $k_c = 0.5$.

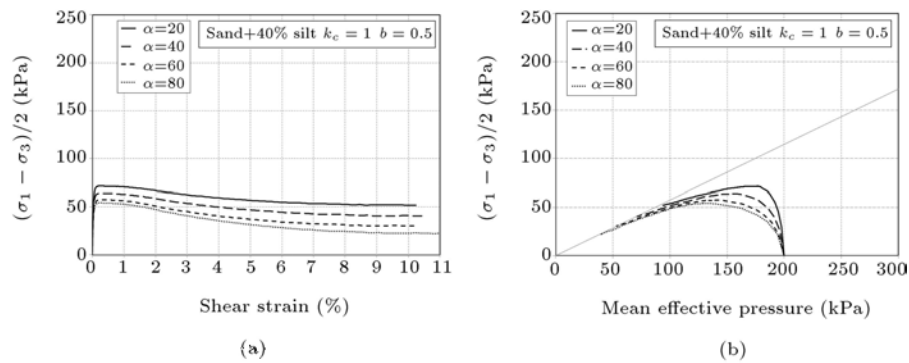


Figure 15. Effect of α on the behavior of Babolsar sand with 40% silt in $P'_c = 200$ kPa and $k_c = 1$.

sand decreases by the increase in silt up the point of separation of sand particle where it starts to increase.

As shown in Figures 6, 9, 12 and 15, by increasing silt content of the material for the specimens consolidated isotropically, the behavior of the material becomes more contractive and usually reaches to the steady state condition without any phase transformation (e.g. Figure 15). Also the same trends can be observed for anisotropically consolidated material with $k_c = 0.33$ and $k_c = 0.5$ as shown in Figures 5, 8, 11 and 14. On the other hand, referring to Table 2, one can observe that increasing silt content in the mixture decrease the strength of the specimen (q_{peak}) and increase the susceptibility to strain softening behavior ($q_{peak} - q_{ini}$). The previous studies by Yamamuro and Covert [30] and Bahadori et al. [12] show that adding silt material to host sand reduces shear strength of the sand. The current study approves this statement. Shear strength of a material decreases by adding silt contents up to 30% silt and then starts to increase by adding more silt to the material for all values of k_c .

The minimum undrained strength at $k_c = 0.33$ is about double of that at $k_c = 1$ when $\alpha \geq 60^\circ$ for sand with different silt contents (e.g. Figures 7 and 9). However for $\alpha \leq 40^\circ$, the ratio of the minimum undrained strengths at $k_c = 0.33$ and $k_c = 1$ is less than 2 (e.g. Figures 10 and 12). This demonstrates that the influence of initial k_c on the minimum undrained

strength of sands is more prominent for higher values of α .

By decreasing k_c , the stress state at the end of consolidation becomes closer to failure line as shown in Figures 7, 10 and 13. So with a slight increase in shear stress for $k_c = 0.33$, stress state reaches to failure line and steady state condition. As a result, the behaviors of highly anisotropic silty sand materials are alike and variation of α has little effect on undrained behavior of highly anisotropically consolidated material. As shown in Figures 4 to 15, for specimens with the same silt contents, decreasing k_c (higher anisotropy) causes the total peak shear strength of sand and silty sand material to increase; however the deviatoric stress required after anisotropic consolidation stress decreases by decrease in k_c as shown in Figure 16.

6. Analysis of the results and discussion

6.1. Initiation of contractive deformation

The degree of strain softening is often characterized by the brittleness index I_B [31], defined as:

$$I_B = \frac{q_{peak} - q_{min}}{q_{peak}}, \tag{10}$$

in which q_{peak} and q_{min} are the peak and minimum undrained deviatoric stress, respectively. I_B is regarded as an indicator of flow potential for strain-

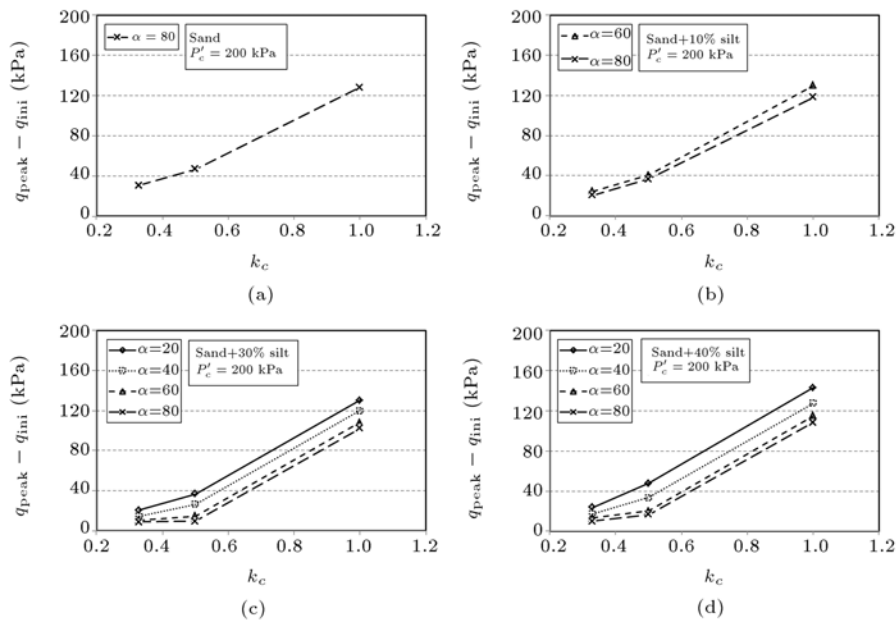


Figure 16. Variation of $q_{peak} - q_{ini}$ with k_c and α for sand and silty sand.

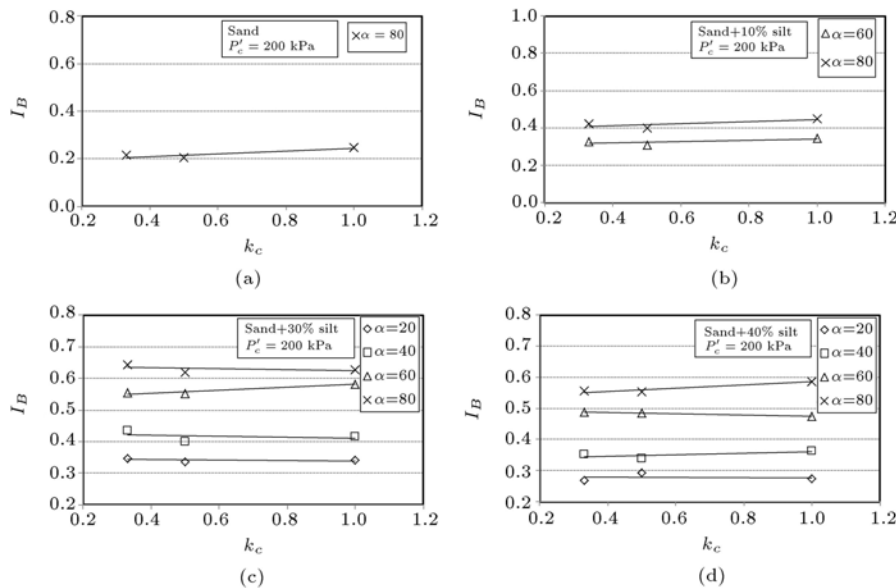


Figure 17. Variation of brittleness index with k_c and α for sand and silty sand.

softening behavior of sands. A considerable increase in I_B was reported by Bahadori et al. [12] and Sivathan and Vaid [16] with increasing α in sands and silty sands.

As shown in Figures 4 to 9, for sand, and sand with 10% silt, respectively, under loading conditions at $\alpha \leq 60^\circ$ and $\alpha \leq 40^\circ$, the reduction in the strength does not occur and I_B in these cases is equal to zero. In other cases, either the quasi steady state or the steady state condition is determined as the minimum strength and the peak points are determined as peak strengths.

Figure 17 shows the variation of I_B against k_c for sand and silty sand material. Increasing anisotropic consolidation or initial shear stress (decreasing k_c) does

not appear to influence I_B significantly and it is almost constant for selected value of α . The variation of average of I_B against α for silty material is shown in Figure 18. An absolute increase in brittleness index can be noted with increasing α especially by increasing silt content of the material up to 30% silt content. Similar results have been reported for sand under compression, extension, shear and principle stress rotation loading [16,27].

The anisotropic consolidated sand and silty specimens with low values of k_c may experience strain softening behavior at high values of α . The steady state strength can be much lower than the initial shear

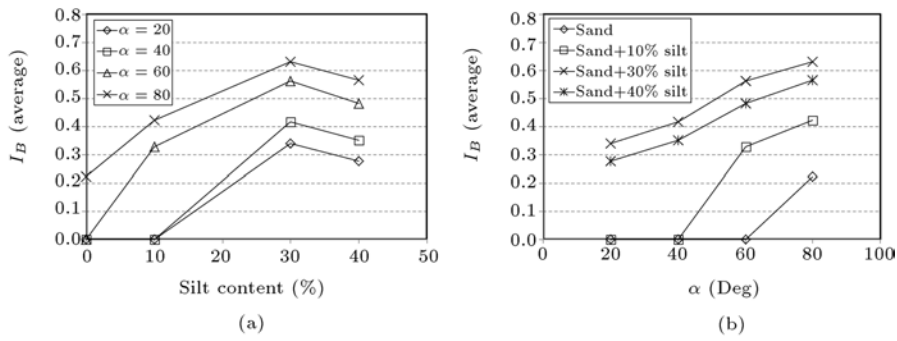


Figure 18. Variation of average brittleness index with silt content and α .

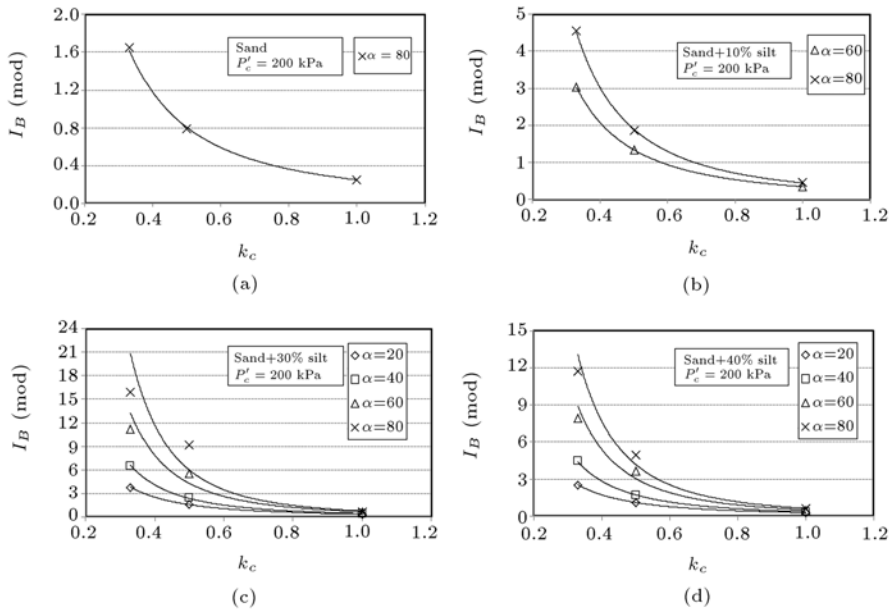


Figure 19. Variation of modified brittleness index with k_c and α for sand and silty sand.

stress. Such a behavior can represent a potential for a flow slide.

Keeping k_c constant and increasing α and the silt content, brittleness index increases but this trend stops at 30% silt. At 40% silty sand, brittleness index decreases with respect to that of 30% silt as shown in Figure 18.

The original definition of brittleness index by Bishop [31] was intended to characterize flow potential of initially hydrostatically consolidated soils. It cannot fully describe flow potential for initially anisotropically consolidated sands. Sivathayalan and Vaid [16] suggested an alternative expression for flow potential of sands at different α and k_c values by considering the peak and the minimum strength values with reference to the initial level of deviatoric stress (q_{ini}) at consolidation stage. This modified brittleness index $I_{B(mod)}$ was defined as:

$$I_{B(mod)} = \frac{q_{peak} - q_{min}}{q_{peak} - q_{ini}} \quad (11)$$

A better characterization is expected for flow potential of anisotropically consolidated sands using modified definition for brittleness index. Figure 19 shows the variation of modified brittleness index against k_c for various amount of α for sand and silty sand material tested in this study. $I_{B(mod)} = 0$ corresponds to no strain softening, and $I_{B(mod)} = 1$ represents minimum undrained strength, which is equals to the initial static shear stress. $I_{B(mod)}$ values larger than 1 imply minimum undrained strength lower than the initial static shear stress, and hence the triggering of a flow slide, if equilibrium is disturbed by a small undrained perturbation. As indicated in Figure 19, the potential of flow increases at high levels of initial shear stress by increasing α . Also adding more silt to host sand increase the rate of increase in $I_{B(mod)}$, that is, the potential of flow of silty sand specimen increases by increasing the silt content up to 30% silt and decrease afterwards.

6.2. Steady-State Friction angle ϕ_{ss}

Undrained tests on sand and silty sand have shown

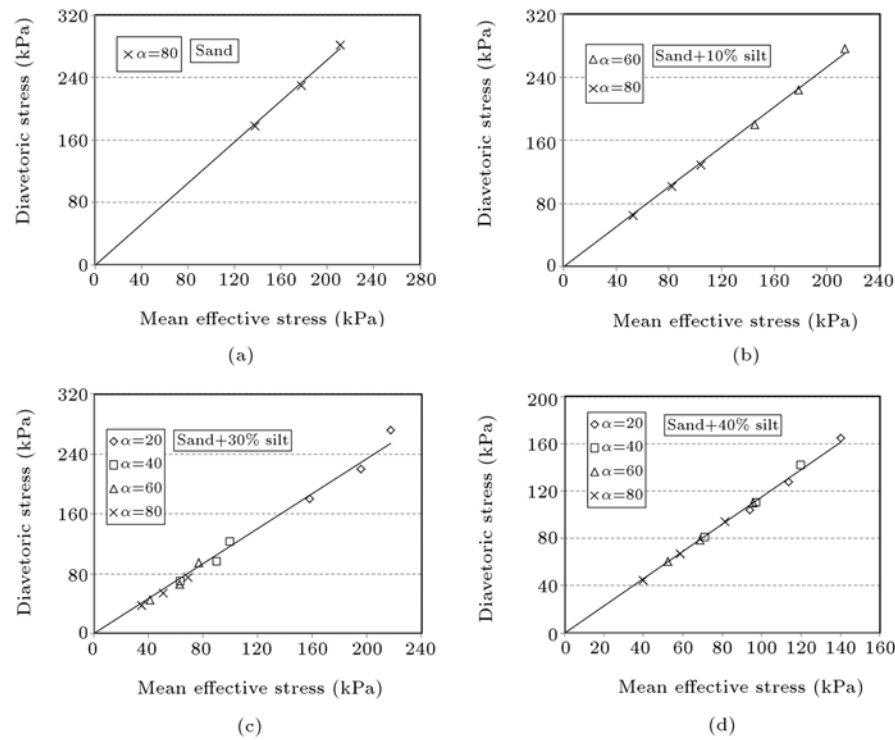


Figure 20. Effective stress conditions at quasi steady state and steady state for Babolsar sand with silt.

that steady state friction angle (or slope of $q - p'$ curve at steady state condition) is a unique parameter for a given sandy soil. This parameter is said to be independent of initial fabric, k_c and α [5]. The condition of steady state at large strains is achieved after complete rearrangement of the sand particles. It should be noted that (for sands) this rearrangement takes place at the shear zone and not at other parts of the specimen. The initial fabric is completely destroyed and due to large strains at constant volume, a new fabric is formed at steady-state. The steady state friction angle (Φ'_{ss}), mobilized at large strains, is a material characteristic which depends only on physical properties such as mineralogy, gradation and the shape of coarse and fine grains of the soil [5]. Steady state friction angle (Φ'_{ss}) may be calculated using Mohr-Coulumb failure criteria (Eq. (12)).

$$\frac{\sigma'_1}{\sigma'_3} = \frac{1 + \sin \phi'_{ss}}{1 - \sin \phi'_{ss}} \quad (12)$$

The principle stresses (σ'_1, σ'_3) can be replaced according to mean effective pressure (P') and induced deviator stress (q). So Eq. (12) can be rewritten as:

$$\sin \phi'_{ss} = \left(\frac{3q}{6p' + q - 2bq} \right)_{ss} \quad (13)$$

$$\sin \phi'_{ss} = \left(\frac{3 \left(\frac{q}{p'} \right)}{6 + \left(\frac{q}{p'} \right) - 2b \left(\frac{q}{p'} \right)} \right)_{ss} = \left(\frac{3M_{ss}}{6 + M_{ss} - 2bM_{ss}} \right)_{ss} \quad (14)$$

where M_{SS} is the slope of $q - p'$ curve in $q - p'$ space in the steady state condition and $p' = (\sigma'_1 + \sigma_2 + \sigma'_3)/3$, $q = (\sigma_1 - \sigma'_3)$. As indicated in Eq. (14), steady state friction angle depends on b . The value of M_{SS} for each type of material is obtained from $q - p'$ curve and the value of steady state friction angle is calculated using Eq. (13). Figure 20 show data from undrained tests plotted in $q - p'$ space. This figure shows that the data associated with different value of α for specimens with 30% and 40% silt contents lie along a straight line passing through the origin, regardless of the initial value of α , k_c , or the mechanism of deformation. However, the steady state happens for 10% silt and clear sand only for high α values. This implies the uniqueness of the steady state in the effective stress space. The value for fitting parameter derived through least squares regression, M_{SS} , and associated steady state friction angle are summarized in Table 3.

As shown in Table 3, the steady state friction angle of the sand decreases with increasing silt content

Table 3. The value of M_{SS} and Φ'_{ss} for different mixtures of Babolsar sand with silt

Silt content (%)	M_{SS}	Φ'_{ss}
0	0.654	40.8
10	0.625	38.7
30	0.564	34.4
40	0.572	34.9

to reach a minimum value at sand with 30% silt. Then the steady state friction angle starts to increase for silty sand material with 40% silt. The present results suggest that the addition of silt in the sand leads to a decrease in Φ'_{ss} . The maximum reduction of Φ'_{ss} is about 16% which happens for sand with 30% silt.

The angularities of the silt particles play an important role on the behavior of silty sand material. Both silt and Babolsar sand which are used in this study were obtained from natural alluvial deposits. Alluvial deposits have usually been eroded and reshaped by water, so their particles have usually rounded and semi-rounded shape with a few semi-angular particles as shown in Figure 21. When shear loading was applied to silty sand specimen, because of shape of silt and sand particles, they can move easily against each other and decrease Φ'_{ss} of the mixture. In contrast, data by Murthy et al. [24] and Sladen et al. [20] showed that the addition of non-plastic crushed silica silt to angular particles increased the average value of Φ'_{ss} . The different angularities of silt and host sand lead to increase the

effect of silt on the Φ'_{ss} . In addition to the angularities of the particles, the method of preparation of specimen has direct effect on the fabric of silty sand mixtures and it should be considered in interpretation of the results.

Decreasing Φ'_{ss} with increasing silt content can physically be explained. When small amount of non-plastic silt fines is added to sand grains, most of the silt particles fill in the voids of sand material. In this condition, the sand skeleton bearing the applied shear load and the sand behavior is dominant. The presence of relatively small amounts of silt between the sand grains makes a sort of smoothing the contacting surface of sands and reduces the shear strength of the fabric of the silty sand. In other words, when the silty sand with small amount of silt is sheared, the weak contacts between sand grains dominate and the shear strength decreases.

6.3. Minimum undrained strength

Figure 22 illustrates the dependence of minimum undrained strength τ_{min} ($q_{min}/2$) on α and k_c for sand

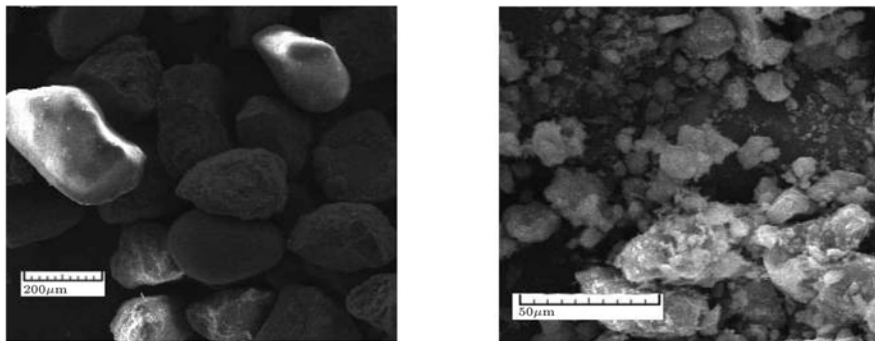


Figure 21. Subrounded Particle of Babolsar sand and subangular particle of silt.

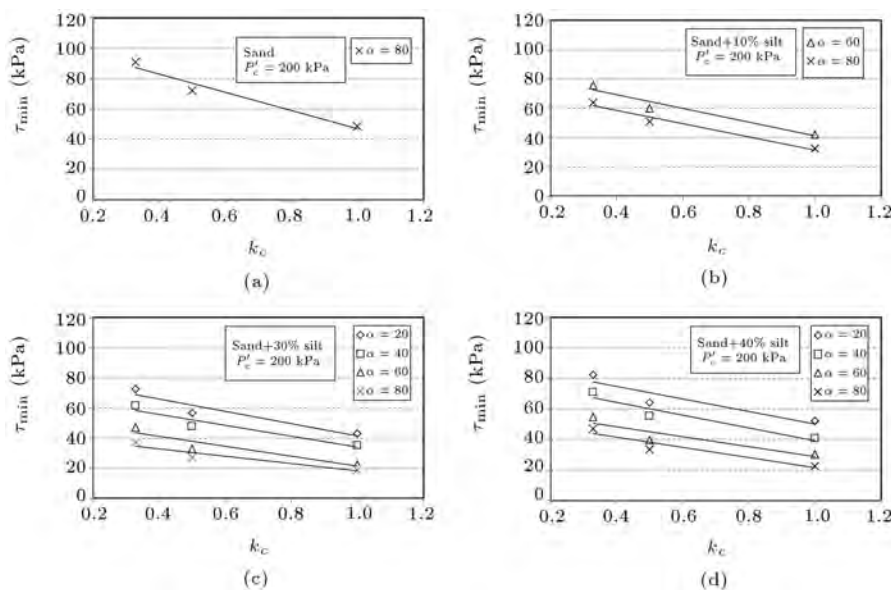


Figure 22. Variation of minimum undrained strength with k_c and α for sand and silty sand.

and silty sand material. The minimum undrained strengths correspond to minimum values of either quasi steady state or steady state conditions for each loading condition on each material. At a given k_c , as depicted in Figure 22, a systematic decrease in minimum undrained strength can be seen with an increase in α , regardless of the type of the material. For a given α , the rate of increase of q_{min} with decrease of k_c (increasing initial static shear stress) is essentially constant for all soils in question (Figure 22). As explained, the minimum undrained strengths are selected according to either quasi steady state or steady state conditions. But both of the quasi-steady state and the steady state are located on one curve and the relationship between τ_{min} and k_c is not dependent on the state of the soil at minimum strength.

In other words, the specimens are initially in drained equilibrium under an anisotropic consolidation stress q_{ini} . Then, the specimen is loaded under undrained conditions, the shearing resistance builds up to a peak value (Figure 16). At that point the specimen becomes unstable and strains rapidly toward the minimum shear strength (τ_{min}) that is smaller than the initial shear stress.

The data shown in Figure 23 is normalized value of Figure 22 by major principal stress at consolidation. As shown in Figure 23, the normalized minimum undrained strength is essentially independent of k_c or initial deviatoric stresses (q_{ini}); however it depends on α . Similar normalized data from previous studies [16] on sand material in triaxial extension and simple shear loading also support this contention. Adding silt content to the host sand does not influence too much the behavior of the host sand in this respect. The relationship between normalized minimum undrained strength and α is linear (the normalized minimum undrained strength decreases with increase in α).

According to the tests results and Figure 23, the location of the lines associated with normalized minimum undrained strength changes for sand with different silt contents, and the minimum values of normalized minimum undrained strength occur for sand with 30% silt content for any α . This fact indicates the dependency of normalized minimum undrained strength on the silt content.

7. Conclusions

A series of undrained tests with using hollow cylinder apparatus were performed on clean and silty sands with nonplastic silt contents ranging from 10% to 40%. Specimens were prepared using wet tamping methods. The main focus of this paper is on the evaluation of the behavior of anisotropic silty sand under a variety of stress path with constant value b during shear stage.

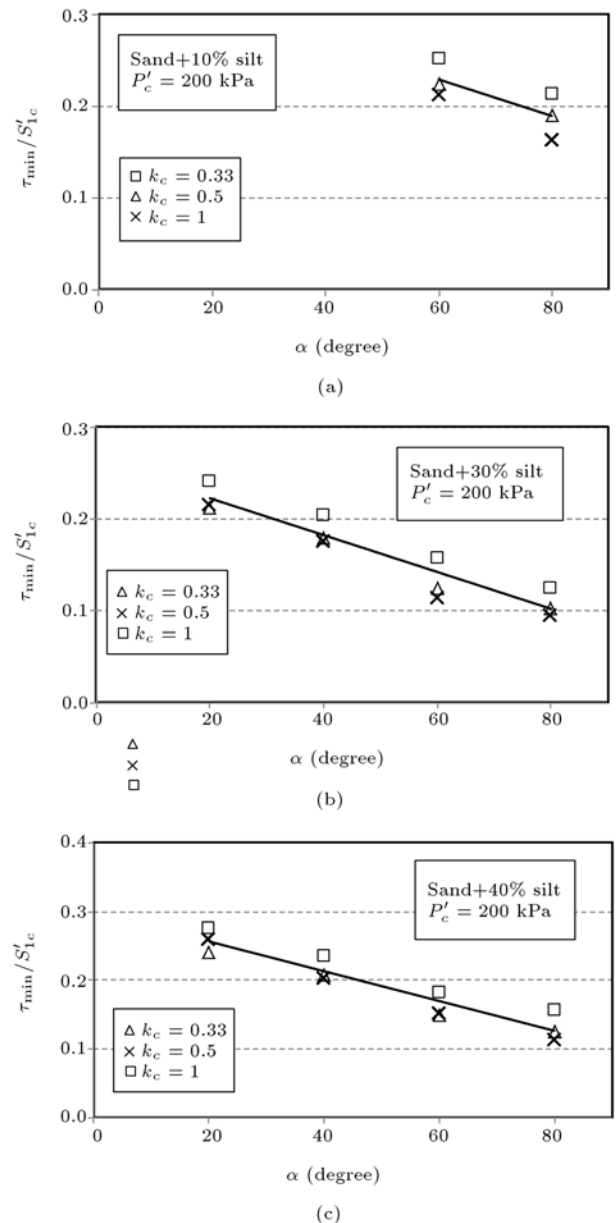


Figure 23. Variation of normalized minimum undrained strength with α for silty sand.

Different states of consolidation stress produce different stress-strain behavior during shearing and hence different excess pore water pressure. In anisotropic consolidation, the stress state at consolidation with $k_c = 0.33$ becomes closer to the failure line and for the same material decreasing k_c causes the minimum shear strength of the material to increase.

Adding silt up to 30% by weight to the sand host reduces the shear strength of the material and then the shear strength increases for sand with 40% silt. In addition adding silt to the sand makes the material weaker and more susceptible to flow.

Applying load with higher α can change behavior of specimen from dilative to contractive and increases

susceptibility to flow. Also silt contents and α have more influence on brittleness index compared to k_c .

The steady state friction angle (Φ'_{ss}) for silty sand with 30% and 40% silt contents is essentially constant and the data associated with different value of α lie along a straight line passing through the origin, regardless of the initial value of α , k_c , or the mechanism of deformation. This implies uniqueness of the steady state in the effective stress space. Also the normalized minimum undrained strength by major principal stress at consolidation appears to be dependent on the loading path and independent from the k_c .

Acknowledgment

Hollow cylinder tests were conducted in the Advanced Geotechnical Engineering Laboratory of Civil Engineering Department of Sharif University of Technology.

References

1. Symes, M.J., Gens, A. and Hight, D.W. "Drained principal stress rotation in saturated sand", *Geotechnique*, **38**(1), pp. 59-81 (1988).
2. Terzaghi, K. "Varieties of submarine slope failures", *Proc., 8th Texas Conf. on Soil Mech. and Found. Engrg.*, Univ. of Texas, Austin, Texas, pp. 29-41 (1956).
3. Kuerbis, R., Negusse, D. and Vaid, Y.P. "Effect of gradation and fine content on the undrained response of sand", *Hydraulic Fill Structure, Geotechnical Special Publication*, **21**, New York, pp. 330-345 (1988).
4. Pitman, T.D., Robertson, P.K. and Sego, D.C. "Influence of fines on the collapse of loose sands", *Canadian Geotechnical Journal*, **31**, pp. 728-739 (1994).
5. Ishihara, K. "Liquefaction and flow failure during earthquake", *Geotechnique*, **43**(3), pp. 351-415 (1993).
6. Verdugo, R. and Ishihara, K. "The steady state of sandy soils", *Soil and Foundation*, **36**(2), pp. 81-91 (1996).
7. Amini, F. and Qi, G.Z. "Liquefaction testing of stratified silty sands", *J. Geotech. and Geoenviron. Engrg., ASCE*, **126**(3), pp. 208-217 (2000).
8. Lade, P.V. and Yamamuro, J.A. "Effects of nonplastic fines on static liquefaction sands", *Canadian Geotechnical Journal*, **34**, pp. 918-928 (1997).
9. Yamamuro, J.A. and Lade, P.V. "Steady-state concept sand static liquefaction of silty sands", *J. Geotech. and Geoenviron. Engrg., ASCE*, **124**(9), pp. 868-877 (1998).
10. Thevanayagam, S. "Effect of fines and confining stress on undrained shear strength of silty sands", *J. Geotech. and Geoenviron. Engrg., ASCE*, **124**(6), pp. 479-491 (1998).
11. Haeri, S.M. and Yasrebi, S.S. "Effect of amount and angularity of particles on undrained behavior of silty sands", *Scientia Iranica*, **6**(3&4), pp. 188-195 (1999).
12. Bahadori, H., Ghalandarzadeh, A. and Towhata, I. "Effect of non plastic silt on the anisotropic behavior of sand", *Soils and Foundation*, **48**(4), pp. 531-545 (2008).
13. Zlatovic, S. and Ishihara, K. "On the influence of nonplastic fines on residual strength", *1st Int. Conf. on Earthquake Geotech. Engrg.*, Rotterdam, Netherlands, pp. 239-244 (1995).
14. Yang, J. and Wei, L.M. "Collapse of loose sand with the addition of fines: the role of particle shape", *Geotechnique*, **62**(12), pp. 1111-1125 (2012).
15. Yoshimine, M., Ishihara, K. and Vargas, W. "Effects of principal stress direction and intermediate principal stress on undrained shear behavior of sand", *Soils and Foundations*, **38**(3), pp. 179-188. (1998).
16. Sivathayalan, S. and Vaid, Y.P. "Influence of generalized initial state and principal stress rotation on the undrained response of sands", *Canadian Geotechnical Journal*, **39**, pp. 63-76 (2002).
17. thayakumar, M. and Vaid, Y.P. "Static liquefaction of sands under multiaxial loading", *Canadian Geotechnical Journal*, **35**, pp. 273-283 (1998).
18. Yang, J. and Sze, H.Y. "Cyclic behaviour and resistance of saturated sand under non-symmetrical loading conditions", *Geotechnique*, **61**(1), pp. 59-73 (2011).
19. Kato, S., Ishihara, K. and Towhata, I. "Undrained shear characteristic of saturated sand under Anisotropic consolidation", *Soils and Foundations*, **41**(1), pp. 1-11 (2001).
20. Sladen, J.A., D'ollander, R.D. and Krahn, J. "The liquefaction of sands, a collapse surface approach", *Canadian Geotechnical Journal*, **22**(4), pp. 564-578 (1985).
21. Haeri, S.M., Noorzad, R. and Oskoorouchi, A.M. "Effect of geotextile reinforcement on the mechanical behavior of sand", *Geotextile and Geomembrane*, **18**, pp. 385-402 (2000).
22. Hight, D.W., Gens, A. and Symes, M.J. "The development of a new hollow cylinder apparatus for investigating the effects of principle stress rotation in soils", *Geotechnique*, **33**(4), pp. 355-383 (1983).
23. Sayao, A. and Vaid, Y.P. "A critical assessment of stress non uniformities in hollow cylinder test specimens", *Soil and Foundation*, **31**(1), pp. 60-72 (1992).
24. Ladd, R.S. "Preparing test specimens using undercompaction", *Geotechnical Testing Journal*, **1**(1), pp. 16-23 (1978).
25. Thevanayagam, S., Shenthan, T., Mohan, S. and Liang, J. "Undrained fragility of clean sands, silty sands and sandy silts", *J. Geotech. and Geoenviron. Engrg., ASCE*, **128**(10), pp. 849-859 (2002).
26. Thevanayagam, S. "Intergrain contact density indices for granular mixes-I: Framework", *J. Earthquake En-*

gineering and Engineering Vibration, **6**(2), pp. 123-134 (2007).

27. Vaid, Y.P. and Sivathayalan, S. "Fundamental factors affecting liquefaction susceptibility of sands", *Canadian Geotechnical Journal*, **37**, pp. 592-606 (2000).
28. Yoshimine, M. and Ishihara, K. "Flow potential of sand during liquefaction", *Soils and Found.*, **38**(3), pp. 189-198 (1998).
29. Murthy, T.G., Loukidis, D., Carraro, J.A.H., Prezzi, M. and Salgado, R. "Undrained monotonic response of clean and silty sands", *Geotechnique*, **57**(3), pp. 273-288 (2007).
30. Yamamuro, J.A. and Covert, K.M. "Monotonic and cyclic liquefaction of very loose sands with high silt content", *Journal of Geotechnical and Geoenvironmental Engineering, ASCE*, **127**(4), pp. 314-324 (2001).
31. Bishop, A.W. "Shear strength parameters for undisturbed and remoulded soil specimens", In *Proceedings of the Roscoe Memorial Symposium*, Cambridge University, Cambridge, Mass., pp. 3-58 (1971).

Biographies

Reza Keyhani received the B.Sc. Degree in Civil Engineering from the Amir Kabir University of Technology, Tehran, Iran, in 1996 and the M.Sc. Degree in Geotechnical Engineering from the Sharif University of Technology (SUT), Tehran, Iran, in 1999. He is currently the PhD candidate in SUT.

He has the first place in Iranian Civil Engineering championship in 1996. His research interests lie in analytical and numerical analysis of earth and rockfill dams and laboratory investigation of soil characterization. He has published 4 Journal and conference

papers. He also has valuable professional experiences in designing large earth and rockfill dam, deep excavation and managing and leading different stages of engineering studies, site investigations and office job.

Seyed Mohsen Haeri received an M.Sc. Degree in Civil Engineering from University of Tehran, Iran in 1977, another M.Sc. Degree in Geotechnical Engineering from University of Illinois at Urbana-Champaign, USA, in 1979, and the PhD degree from Imperial College of Science and Technology, London, UK in 1988. He is Professor of Civil Engineering and currently is the Director of the Geotechnical Engineering Studied and Research Center of Sharif University of Technology (SUT), Tehran, Iran.

Previously he served as the Chairman of Civil Engineering Department and the Director of Earthquake Engineering Research Center of SUT. His research interests lie in the areas of earthquake geotechnical engineering, static and dynamic behavior and characterization of earth and rockfill dams, soil characterization especially for cemented gravelly sands and unsaturated collapsible soils, and implementation of neural network and neuro-fuzzy in geotechnical engineering problems and he has accomplished several national research projects. Prof. Haeri has supervised several PhD and MSc students and has published more than 30 Journal and more than 90 conference papers. He has also published 6 books in Persian. Being consultant to many important engineering projects especially large dams and deep excavations, he has been member of several national committees on various civil engineering issues as well.